

A NUMERICAL STUDY ON THE EFFECT OF GEOMETRIC VARIATION ON ANEURYSM

JAYDEEP CHANDRA SAHU^{a1} AND SOMNATH CHAKRABARTI^b

^{ab}Department of Mechanical Engineering, Indian Institute of Engineering Science and Technology, Shibpur, Howrah,, West Bengal, India

ABSTRACT

An aneurysm is a localized, blood-filled balloon-like bulge in the wall of a blood vessel. It is a cardiovascular health disease that occurs when the blood vessel becomes weak. Aneurysms can occur in any blood vessel commonly seen in artery of circle of Willis in the brain, aortic aneurysm affecting the thoracic aorta and abdominal aortic aneurysm. Aneurysm rupture is a complex phenomenon, depending on the maximum diameter, locally varying mechanical properties of arterial wall, distribution of internal pressure, wall stress, asymmetry, saccular index, presence of intraluminal thrombus, and tortuosity etc. The dilation of aneurysm and the risk of rupture depend on a complex interplay between hemodynamic stresses and biomechanical reactions occurring inside the arterial wall, which are affected by blood flow patterns. The blood flow patterns in aneurysm are affected by the change in geometry of aneurysm. Thus, the flow pattern related to various geometrical aspects of aneurysm need to characterise for better understanding the cause and characteristics of the disease. This study is focusing on abdominal aortic aneurysm. In the present work, an effort has been made to numerically predict the flow characteristics of blood, related to risk of rupture for two dimensional, rigid aneurysm models with variation of Reynolds number ranging from 50 to 400 and Length ratio ranging from 0.5009 to 1.996. The commercial CFD (computational fluid dynamics) software ANSYS 14.5 (FLUENT) is used to design the computation field, meshing and further post-processing. The different hemodynamic factors like streamline contour, wall static pressure distribution and wall shear stress characteristics at the potential locations are investigated. From the flow simulation, it is observed that the flow through an aneurysmal artery consists of two main parts, a high velocity flow in the middle of the geometry with slow recirculation bubbles in the area of the aneurysm cavity. This condition may increase the blood residence time and so the thrombus formation. A peak wall static pressure and peak wall shear stress gradient are found at distal end of aneurysm. The peak static pressure can be the cause of further dilation of arterial wall. The elevated level of wall shear stress may lead to damage of endothelial wall of distal end of aneurysm. It is found that posterior bulging, i.e. greater length ratio leads to increment in peak wall shear stress and maximum wall static pressure at distal end. The magnitudes of peak wall shear stress and maximum wall static pressure are having linearly varying nature with increase in Reynolds number.

KEYWORDS: Aneurysm, CFD, Reynolds Number, Length Ratio, Wall Shear Stress, Streamline Contours, Wall Static Pressure.

An aneurysm is abnormal local dilation in the blood vessel due to weakness in blood vessels, generally if bulging diameter is greater than 50% of its normal diameter. It is considered to be one of the important cardiovascular diseases. An aneurysm may occur as the result of a hereditary condition or aortic disease. Aneurysms are little known among the common human being but they are considered to be a significant cause of mortality. Fifteen thousand people per year die from Abdominal Aortic Aneurysms (AAAs) rupture in the United States alone, making it the 13th leading cause of death in that country and affecting 1 in 250 individuals over 50 years of age [1].

In current medical practices, the maximum size of bulge section is seen as prime factor to decide for further medical intervention. Many literatures have reported that the aneurysm with same maximum diameter can have different shape, varying wall thickness and different mechanical properties of arterial wall [2]. These factors can affect their growth and tendency to rupture. The occurrence of aneurysm and

progression towards rupture is a complex phenomenon, and based on one parameter or two simple parameters to decide the rupture risk is insufficient. Recently, the hemodynamic stresses and arterial wall dynamics are seen as reliable parameters to assess the risk of rupture of arterial wall [3].

In the steady flow approach, Finol and Amon [3] have studied the blood flow patterns and hemodynamic stresses in AAAs. They have considered a two-aneurysm, axisymmetric, rigid wall AAA model for the range of Reynolds numbers $10 < Re < 2265$. They have found that the wall pressure remains constant along the aneurysm and then it takes a peak value at the flow reattachment point. For greater insight into the effects of asymmetry and wall thickness in AAA rupture risk analysis, Scotti et al. [1] have done fully coupled fluid structure interaction (FSI) simulation. From the obtained results, they have pointed out that an asymmetric AAA with regional variations in wall thickness offers higher mechanical stresses and an increased risk of rupture than that of a

more fusiform AAA with uniform wall thickness. To evaluate the importance of shape and geometric variation in aneurysm, Li and Kleinstreuer [4] have numerically analyzed asymmetric aneurysms of the abdominal aorta under the transient 3-D blood flow condition. They have pointed out that the assumption of symmetric AAA geometry may underestimate AAA-wall stress and hence rupture risk assessment. Qing et al. [5] have studied influence of aneurysm geometry on flow hemodynamic. From numerical results, they have seen that aspect ratio is having more impact on flow hemodynamic compared to sac diameter. They have observed that as the aspect ratio (ratio between sac height and neck width) increases, the average wall shear stress (WSS) significantly reduces. The wall pressure enhances and finally intensifies the aneurysm. In order to develop more combined relations between geometric and hemodynamic factors for better clinical decisions, Nair P. et al. [6] have simulated numerical flows within eight idealized template geometries in cerebral aneurysms (CAs). They have concluded that the combination of large dome size and small dome-to-neck ratio (i.e. large, wide-neck terminus aneurysms) produces the most extreme hemodynamic environments encountered in the study. A numerical simulation has been done to find the curvature effect of artery on aneurysm by Halabian et al. [7]. They have observed that the aneurysm preferably develops and progresses at curved arteries. Further they have stated that the curvature can cause flow irregularity, such as flow shift, flow recirculation, secondary flow and oscillating WSS.

In the present work, an effort has been made to numerically predict the flow characteristics of blood, related to risk of rupture for two dimensional, rigid aneurysm models with variation of Reynolds number and Length ratio (LR).

MATHEMATICAL FORMULATION

Governing Equations

A schematic diagram of computational domain of flow through axisymmetric artery is illustrated in Fig.1. The flow under consideration is assumed to be steady, two-dimensional and laminar. The fluid (blood) is taken as incompressible and Newtonian. The geometry of artery is considered as symmetric about central axis and having rigid wall. The density of blood and viscosity are taken as 1050 Kg.m^{-3} and 0.00319 Pa.s respectively [8]. In the computational domain plot of Fig.1, D is the normal artery diameter, H is the maximum height of bulge section, L1 is axial length from inlet of bulge section to maximum bulge section,

L2 is axial length from maximum bulge section to exit of bulge section and L is the total axial length of bulge section. The length ratio (LR) is defined as the ratio between L1 and L2, i.e. $LR = \frac{L1}{L2}$. In our study, three different length ratios i.e. 0.5009, 1.0 and 1.996 for case 1, case 2 and case 3 respectively have been considered for analysis. The normal artery diameter (D) and maximum bulge section height (H) have been kept constant in this study.

The different dimensions under consideration are as follows,

Case 1

D = 20mm [9], L1 = 40mm, L2 = 40mm, H = 3D = 60mm, L = L1+L2 = 4D = 80mm [9], LR = 1.0.

Case 2

D = 20mm, L1 = 26.70mm, L2 = 53.30mm, H = 60mm, L = L1+L2 = 80mm, LR = 0.5009.

Case 3

D = 20mm, L1 = 53.30mm, L2 = 26.70mm, H = 60mm, L = L1+L2 = 80mm, LR = 1.996.

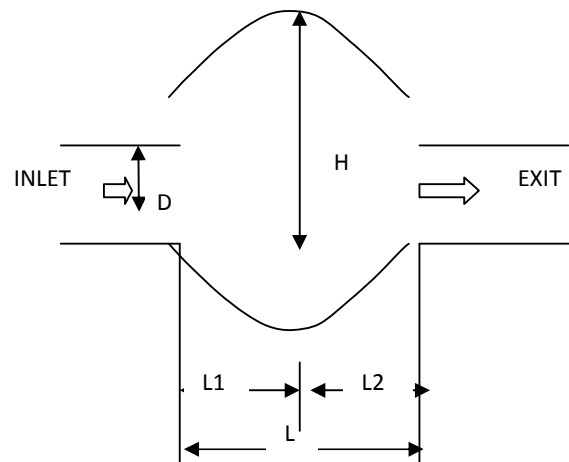


Figure 1: Schematic illustration of computational domain.

General governing equations for flow in arteries are given below,

$$\text{Continuity equation: } \frac{1}{r} \frac{\partial(r u_r)}{\partial r} + \frac{\partial u_z}{\partial z} = 0 \quad (1)$$

Momentum equation in z- axis direction (axial):

$$\rho \left(u_r \frac{\partial u_z}{\partial r} + u_z \frac{\partial u_z}{\partial z} \right) = - \frac{\partial p}{\partial z} + \mu \left[\frac{1}{r} \frac{\partial}{\partial r} \left(r \frac{\partial u_z}{\partial r} \right) + \frac{\partial}{\partial z} \left(\frac{\partial u_z}{\partial z} \right) \right] \quad (2)$$

Momentum equation in r- direction (Radial):

$$\rho \left(u_r \frac{\partial u_r}{\partial r} + u_z \frac{\partial u_r}{\partial z} \right) = -\frac{\partial p}{\partial r} + \mu \left[\frac{1}{r} \frac{\partial}{\partial r} \left(r \frac{\partial u_r}{\partial r} \right) + \frac{\partial}{\partial z} \left(\frac{\partial u_r}{\partial z} \right) - \frac{u_r}{r^2} \right] \quad (3)$$

Boundary Conditions

The following three boundary conditions are applied to present problem. They are as follows,

- (i) At the walls: No slip condition, i.e. $u_z = 0$, $u_r = 0$.
- (ii) At the inlet: Axial velocity has been specified and the transverse velocity has been set to zero, i.e. u_z = specified, $u_r = 0$.
- (iii) At the exit: Constant pressure = 100 mm of Hg (13332.2 Pa) [4].

Numerical Procedure

Commercial software package ANSYS 14.5 (FLUENT) is used to design the computation field and further for meshing. The momentum equations and continuity equation are solved by employing the control volume technique on a uniform staggered grid following SIMPLE algorithm. The discretization of convective terms is done by second order upwind scheme. The convergence of the iterative scheme is achieved when the normalized residual of mass and momentum equations summed over the entire calculation domain falls below 10^{-6} .

In this investigation, WSS is used to illustrate grid independence aspect. Fig.2 illustrates the comparison of wall shear stress at $Re = 400$, for the case 1, i.e. $LR = 1$. In this study, three different set of quadrilateral elements of 72991, 114716 and 137316 are selected for grid independence test. From the WSS plot of Fig.2, it can be seen that a similar trend of WSS magnitude at inlet of artery to the exit of bulge section for the quadrilateral elements of 72991, 114716 and 137316. The magnitude of WSS for quadrilateral element of 72991 shows lower WSS magnitude compared to quadrilateral element of 114716 and 137316. The quadrilateral elements of 114716 and 137316 are having similar trend and same order of magnitude of WSS. The magnitude of WSS is noted to become stabilized as there is a very small variation in curves. In this study, quadrilateral elements of 137316 is looked to be more optimum and in safer side. Finally, the grid element of 137316 has been selected for further simulation work.

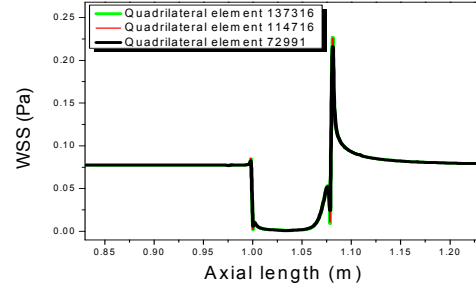


Figure 2: Comparison of WSS for different quadrilateral elements at $Re = 400$ for $LR = 1$ (i.e., case 1).

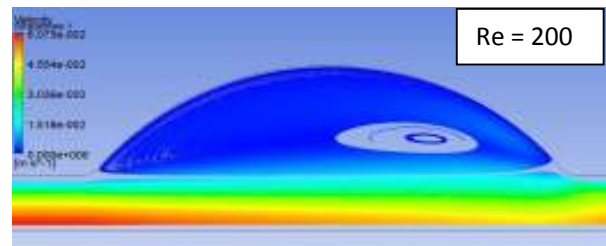
RESULTS AND DISSCUSION

The important results of present study are presented in this section. The parameters of this study are as follows,

Reynolds numbers for the simulation are ranging from 50 to 400 for three different length ratios.

Effect of Reynolds number and length ratio on Streamline Contours

The streamline contour plots are shown in Fig.3, Fig.4 and Fig.5 for LR equal to 1.0, 0.5009 and 1.996 respectively for typical Re of 200 and 400. From the flow simulation, it can be seen that in all the cases the flow through an aneurismal artery consists of two main parts, a high velocity flow in the middle of the geometry with slow recirculation bubbles in the area of the aneurysm cavity. The high velocity region is similar in all models but the recirculation part varies as Re increases from 200 to 400. It has been observed that as the Reynolds number increases from 200 to 400 the vortex become skewed, the centre of circulating flow regions moves downstream toward the distal end of the aneurysm and closer to main stream. This mechanism can be explained by the fact that the diverging shape of the model produces deceleration of the flow, results in very small velocity near the wall of the aneurysm. As the velocity of particles near the wall is small, the particles cannot overcome the high downstream pressure. This creates a recirculation flow near the wall of aneurysm.



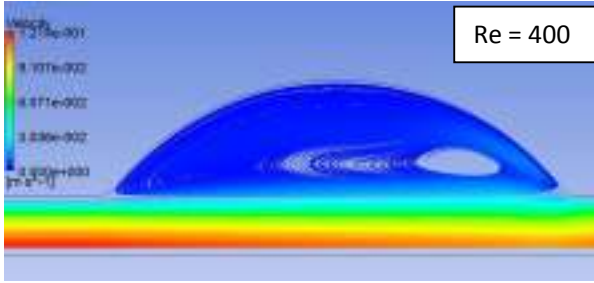


Figure 3: Stream line contours for Re of 200 and 400 for case 1, LR = 1.

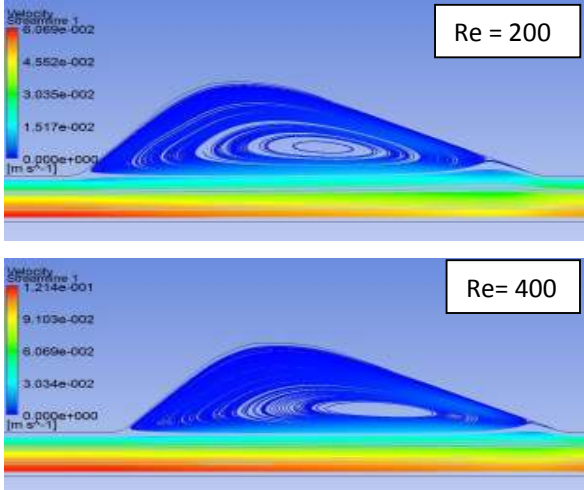


Figure 4: Stream line contours for Re of 200 and 400 of case 2, LR = 0.5009.

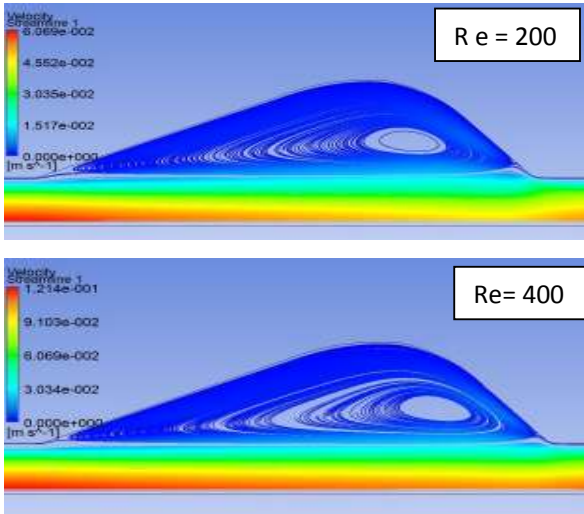


Figure 5: Stream line contours with Re of 200 and 400 for case 3, LR = 1.996.

Further, it is observed that for the case of anterior bulging (LR = 0.5009) i.e. case 2, recirculation vortex are noted to become flattened in axial direction as Re increases from 200 to 400 in comparison to case 1. This leads to wider area of recirculation region near

the wall and probably increases the residence time of blood. While in case of posterior bulging (LR = 1.996) i.e. case 3, the recirculation vortex is noted to become flattened in radial direction and situated near the distal end as Re increases from 200 to 400.

The streamline flows do not produce stresses that lead to aneurysm expansion or rupture. However, they are strongly related to conditions that promote thrombus formation on the artery wall. The thrombus covers the weak artery wall which can provide some support to the weakened wall. However, the thrombus formation may degrade the endothelial layer by imposing restriction on oxygen transport to inner artery wall [10].

Effect of Reynolds number and length ratio on wall static pressure

Fig.6, Fig.7 and Fig.8 show the effect of flow Reynolds number on wall static pressure (WSP) for length ratio (LR) 1, 0.5009 and 1.9929 respectively. Variations for 8 different Reynolds number viz. 50, 100, 150, 200, 250, 300, 350 and 400 are shown here.

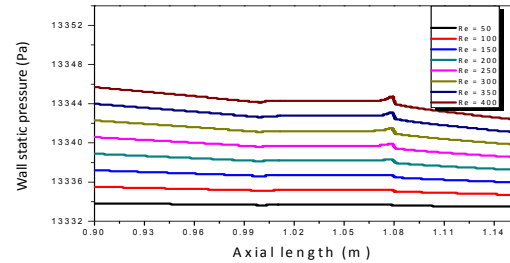


Figure 6: Variation of WSP with Re in axial direction for case 1, LR = 1.0.

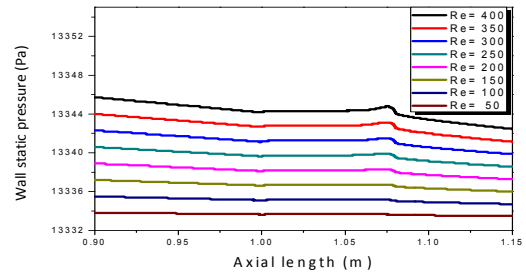


Figure 7: Variation of WSP (Pa) with Re in axial direction for case 2, LR = 0.5009.

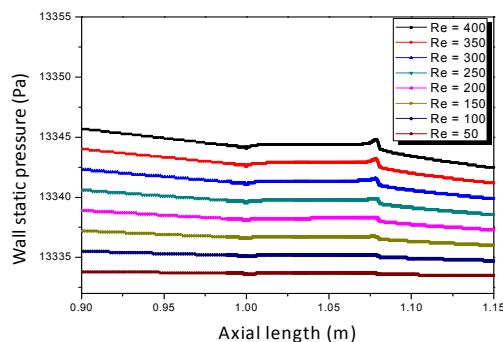


Figure 8: Variation of WSP (Pa) with Re in axial direction for case 3, LR = 1.996.

For all the cases, the pressure reaches to a minimum value at the separation point and increases gradually along the aneurysm. Then the pressure reaches to a maximum magnitude at the distal end near to reattachment zone and declines sharply after the distal end of the aneurysm. It is also found that the maximum wall static pressure at the distal end increases with increase in flow Reynolds number.

The pressure distribution results indicate that once an aneurysm is formed, the fluid dynamics inside the cavity will increase the pressure, further dilating the aneurysm. For this the wall thickness decreases with the increase in the level of disease aneurysm. The peak wall static pressure, at the zone of reattachment point may exceed the wall stress strength and it may lead to rupture of the aneurysm.

Effect of Reynolds number and length ratio on wall shear stress

Fig.9, Fig.10 and Fig.11 show the effect of flow Reynolds number on wall shear stress (WSS) for length ratio (LR) 1.0, 0.5009 and 1.996 respectively. Variations for 8 different Reynolds number viz. 50, 100, 150, 200, 250, 300, 350 and 400 have been considered to present the outcome of simulation. Further, Fig.12 demonstrates the effect of Re on maximum and minimum WSS for the length ratios considered in three cases.

For all the cases of Fig.9, Fig.10 and Fig.11, it is noted that the WSS decreases rapidly to zero at the separation point. It maintains a low value, because of the flow reversal in the recirculation zone along the aneurysm. Then, the wall shear stress rises sharply to a peak value near to the reattachment point. It is also noted that as Reynolds number increases, the magnitude of peak wall shear stress increases. This mechanism can be explained by the fact that due to convective deceleration of the flow, the velocity decreases in the

proximal half of the aneurysm, which results in a decrease in the wall shear stress to a zero value at the point of separation. Similarly, the shear stress value at the distal end is also zero because of the site of boundary layer reattachment. The wall shear stress value increases sharply after the point of reattachment because the velocity increases sharply due to the convective acceleration. So, the vicinity of the reattachment point is a site of localized low and high positive wall shear stresses for all the Reynolds number.

From Fig.12, It has been observed that the maximum wall shear stress increases with increase in length ratio. This can be explained by the fact that as the LR increases from 0.5009 to 1.996, the velocity gradient increases at the distal end because the recirculation vortexes are noted to flatten in radial direction. This flattening effect leads to higher WSS at distal end.

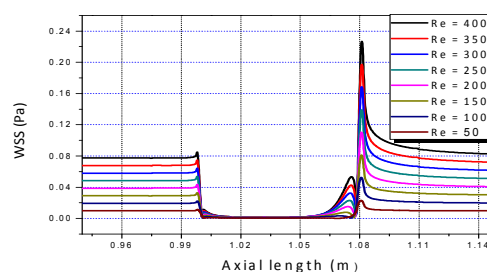


Figure 9: Variation of WSS (Pa) with Re in axial direction for case 1, LR = 1.0.

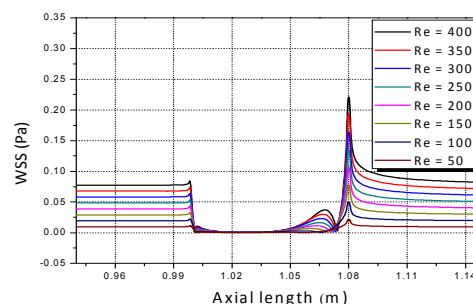


Fig.10: Variation of WSS (Pa) with Re in axial direction for case 2, LR = 0.5009.

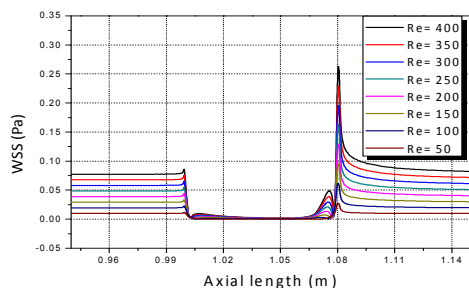


Figure 11: Variation of WSS (Pa) with Re in axial direction for case 3, LR=1.996.

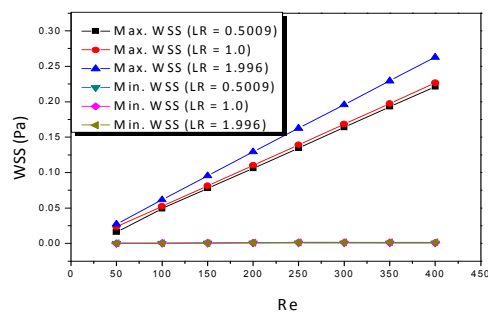


Figure 12: Variation of maximum WSS (Pa) and minimum WSS (Pa) with the variation of Re for different LR.

The wall shear stress distribution along the aneurysm shows the main mechanism of deposition of platelets and blood clotting along the wall of aneurysm. The peak WSS occurs at the reattachment zone. It activates platelets approaching this zone which get entrapped into recirculation zone. Once trapped into the recirculation region, they experience low WSS for prolong time leading to adhesion of platelets into the artery wall, causing thrombus formation [10].

CONCLUSION

In present work, a numerical study on flow characterization through rigid wall aneurysm model for three cases, case 1, case 2 and case 3 i.e. length ratio 1.0, 0.5009 and 1.996 have been carried out. Reynolds numbers for the flow simulation are ranging from 50 to 400. It leads to following observations.

1. As the Reynolds number increases from 200 to 400 the vortex becomes skewed and the centre of circulating flow regions moves downstream toward the distal end of the aneurysm for all LR. For LR = 0.5009, vortex is skewed in axial direction as Re increases from 200 to 400, promoting the thrombus formation inside the aneurysm. In case of LR = 1.996, vortex becomes flattened in radial direction with increase in Re from 200 to 400.

2. For all the cases, the pressure reaches to a minimum at the separation point and increases gradually along the aneurysm. Then the pressure reaches to a maximum value near the reattachment zone and declines sharply after the distal end of the aneurysm. As the static pressure increases in aneurysm cavity, it leads to further dilation of the aneurysm cavity.

3. For all the cases, it is noted that as Reynolds number increases the value of peak wall shear stress increases. This peak WSS may lead to damage of endothelium layer at distal end of aneurysm. As the length ratio increases, the magnitude of maximum WSS enhances. This implies that posterior bulging is having more prone to rupture compared to other cases.

REFERENCES

- Scotti C. M., Shkolnik A. D., Muluk S. C. and Finol E. A., 2005. "Fluid-structure interaction in abdominal aortic aneurysms: effects of asymmetry and wall thickness," *BioMedical Engineering OnLine*, **4**.
- Vorp D. A., Raghavan M. L. and Webster M. W., 1998. "Mechanical wall stress in abdominal aortic aneurysm: Influence of diameter and asymmetry," *Journal of vascular surgery*, **27**:632-639.
- Finol E. A. and Amon C. H., 2002. "Flow-induced wall shear stress in abdominal aortic aneurysms: Part I - steady flow hemodynamics," *computer Methods in Biomechanics and Biomedical Engineering*, **4**:309-318.
- Li Z. and Kleinstreuer C., 2007. "A comparison between different asymmetric abdominal aortic aneurysm morphologies employing computational fluid-structure interaction analysis," *European Journal of Mechanics, Biomedical Fluids*, **26**:615-631.
- Qing W. and Wei-zhe W., 2009. "Simulation of blood flows in intracranial ICA-Pcoma aneurysm via computational fluid dynamics modeling," *Journals of Hydrodynamics*, **21**:583-590.
- Nair P., Chong W. B., Indahlastari A., Lindsay J., DeJeu D., Parthasarathy V., Ryan J., Babiker H., Workman C., Gonzalez L. F. and Frakes D., 2016. "Hemodynamic characterization of geometric cerebral aneurysm templates," *Journal of Biomechanics*, **49**:2118-2126.
- Halabian M., Karimi A., Beigzadeh B. and Navidbakhsh M., 2015. "A numerical study on

the hemodynamic and shear stress of double aneurysm through s shaped vessel,” Biomedical Engineering: Applications, Basis and Communications, **27**:1550033-1-10.

Canchi T., Kumar S. D., Ng E. Y. K. and Narayanan S., 2015. “A review of computational methods to predict the risk of rupture of abdominal aortic aneurysms,” Hindawi Publishing Corporation, BioMed Research International Volume.

Paramasivam V., Filipovic N., Muthusamy K. and Kadir M. R. A., 2010. “Finite element modelling for solving pulsatile flow in a fusiform abdominal aortic aneurysm,” Biomedicine International, **1**:50-61.

Sheard G. J., 2009. “Flow dynamics and wall shear-stress variation in a fusiform Aneurysm,” J Eng Math, **64**:379-390:2009.

Stamatopoulos C., Papaharilaou Y., Mathioulakis D. S. and Katsamouris A., 2010. “Steady and unsteady flow within an axisymmetric tube dilatation,” Experimental Thermal and Fluid Science, **34**:915-927.